International Journal of Advanced Science and Technology
Vol. 29, No. 8, (2020), pp. 1017-1025

Cognitive Artificial-Intelligence for Rogers Ratio Dissolved Gas Analysis

Karel Octavianus Bachri[1*], Tajuddin Nur[2], Umar Khayam[3], Bambang Anggoro Soedjarno[4], Arwin Datumaya Wahyudi Sumari[5]
[1, 2]*Atma Jaya Catholic University of Indonesia, Jakarta, Indonesia*
[3, 4]*Bandung Institute of Technology, Bandung, Indonesia*
[5]*State Polytechnic of Malang, Malang, Indonesia*
Email: [1]karel.bachri@atmajaya.ac.id, [2]tans@atmajaya.ac.id, [3]umkha@yahoo.com, [4]b.anggoro55@yahoo.com, [5]arwin.sumari@polinema.ac.id

Abstract

This paper discusses Cognitive Artificial Intelligence (CAI) method for Dissolved Gas Analysis (DGA) interpretation adopting Rogers Ratio method. CAI grows its knowledge through the interaction with its surroundings. Informations are extracted from multiple sources of data and are then fused to obtain new information with Degree of Certainty (DoC). The new information indicates the fault occurred before the observation took place. The proposed method CAI is validated using the IEC TC10 dataset and compared to the conventional Artificial Intelligence Fuzzy Inference System (FIS) and Artificial Neural Network (ANN). Compared to other methods, CAI performs the most accuracy in identifying Low-Energy Discharge (LE) and Thermal-High (TH), while FIS performs the most accuracy in identifying High-Energy Discharge (HE), and ANN performs the most accuracy in identifying Partial Discharge (PD) and Thermal-Low (TL).

Keywords: *Cognitive Artificial-Intelligence, Rogers Ratio, DGA Interpretation, Information Fusion,*

1. Introduction

Electrical power systems consist of generation, transmission, and distribution [1]. Power is generated and transmitted in the form of high-voltage signal to maximize efficiency [2]–[4] and is distributed in the form of low-voltage signal to ensure safety [5], [6]. Transformers change voltage levels using electromagnetic induction principle [1], [7], and thus, the essential part in power systems.

One of the transformer components is oil. Transformer oil has at least three main functions, it provides insulation, dielectric, and acts as coolant [1]. Transformer oil is decomposed during operation due to the presence of stresses [8], radices are released hydrocarbons are formed [8].

Dissolved Gas Analysis (DGA) is used to analyze the composition of dissolved gases in transformer oil to detect faults that might have occurred in a transformer. is Dissolved Gas Analysis (DGA). In our prior research, Doernenburg Ratio Method (DRM) was adopted and resulting 98.02% overall accuracy [9].

While DRM uses more indication [9], Rogers Ratio Method (RRM) accommodates more Possible Faults (PF). RRM uses three Ratios, R_1, R_2, and R_5. Conventional RRM for key gases is shown in Table 1, while its flowchart is shown in Figure 1, has some disadvantages, there are undefined condition after some decisions [10].

ISSN: 2005-4238 IJAST

Table 1. Rogers Ratio for Key gases [10].

Case	R_2	R_1	R_5	Result
0	<0.1	>0.1 to <1	<1	Normal
1	<0.1	<0.1	<1	PD/LE
2	0.1 to 3	0.1 to 1	>3	HE
3	<0.1	>0.1 to <1	1 to 3	TL
4	<0.1	>1	1 to 3	TL/TH
5	<0.1	>1	>3	TH

This can be overcome using Cognitive Artificial Intelligence (CAI). CAI acts based on the information fusion principle, which fuse multi indication with other information to produce new information. The new information is then used to make decision regarding which fault had occurred before the observation.

Comparison between RRM and DRM is shown in Table 2. RRM uses R_1, R_2, and R_5, while DRM uses R_1, R_2, R_3, and R_4. RRM has more detail in thermal faults distinction and less detail in electrical faults distinction. DRM has more detail in electrical faults distinction and less detail in thermal faults distinction.

2. Research Method

Research method can be described as follow:

a. Data collecting: Data are collected from IEC TC10 [11], a labelled dataset that are put into groups: Partial Discharge (PD), Low-Energy Discharge (LE), High-Energy Discharge (HE), Thermal-Low (TL), and Thermal-High (TH).

b. Preprocessing: Data are preprocessed to extract the information using RRM standard. Extraction process produces localized ratio.

c. Information fusion: Localized ratios are fused with RRM standard to produce fused information containing the probability of each PF considering only a single indication, the result will be arranged in Observation Matrix.

d. ASSA2010 inferencing: The system will then calculate the probability of every PF considering all indication in the form of DoC.

e. Estimation: Determming fault based on DoC value.

Table 2. Comparison between RRM and DRM

Comparison	RRM	DRM
Indication	R_1, R_2, and R_5	R_1, R_2, R_3, and R_4
Thermal Faults	More detail	less detail
	(TL, TM, and TH)	(Uses TD for all Thermal Faults)
Electrical Faults	Less detail	More detail
	PD/LE, HE	PD, LE, HE

The normal RRM uses three gas concentration Ratios that is calculated using equation (1) to (3) and works based on Figure 1.

$$\square_1 = [\square\square_4]/[\square_2] \quad (1)$$

$$\square_2 = [\square_2\square_2]/[\square_2\square_4] \quad (2)$$

$$\square_5 = [\square_2\square_4]/[\square_2\square_6] \quad (3)$$

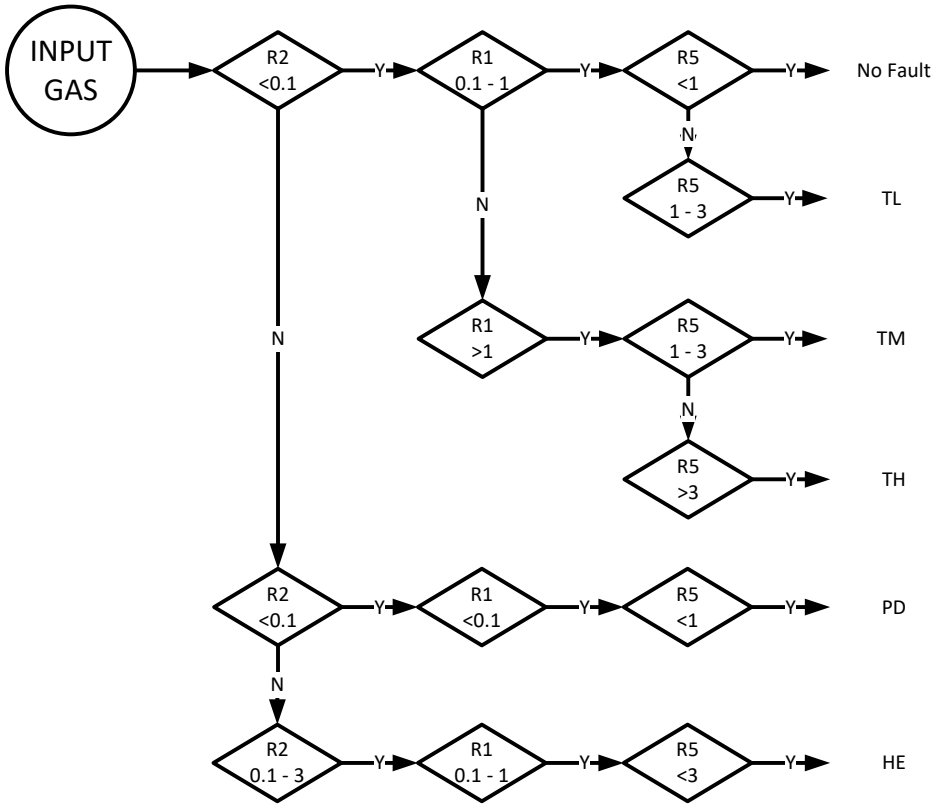

Figure 1. Conventional RRM Flowchart [10]

Input gas will first be put in vials and analyzed with gas chromatogram. R_1, R_2, and R_5, are calculated. If $R_2 < 0.1$, R_1 is more than 0.1 and less than 1.0, and $R_5 < 1.0$, the unit is considered normal. If $R_2 < 0.1$, $R_1 < 0.1$, and $R_5 < 1.0$, the PF is considered PD/LE. If R_2 lies between 0.1 and 3, R_1 lies between 0.1 and 1, and $R_5 > 3$, the PF is considered HE. If $R_2 < 0.1$, R_1 is more than 0.1 and less than 1, and R_5 lies between 1 and 3, the PF is considered TL. If $R_2 < 0.1$, $R_1 > 1$, and $R_5 > 3$, the PF is considered TH.

Proposed method diagram is shown in Figure 2.

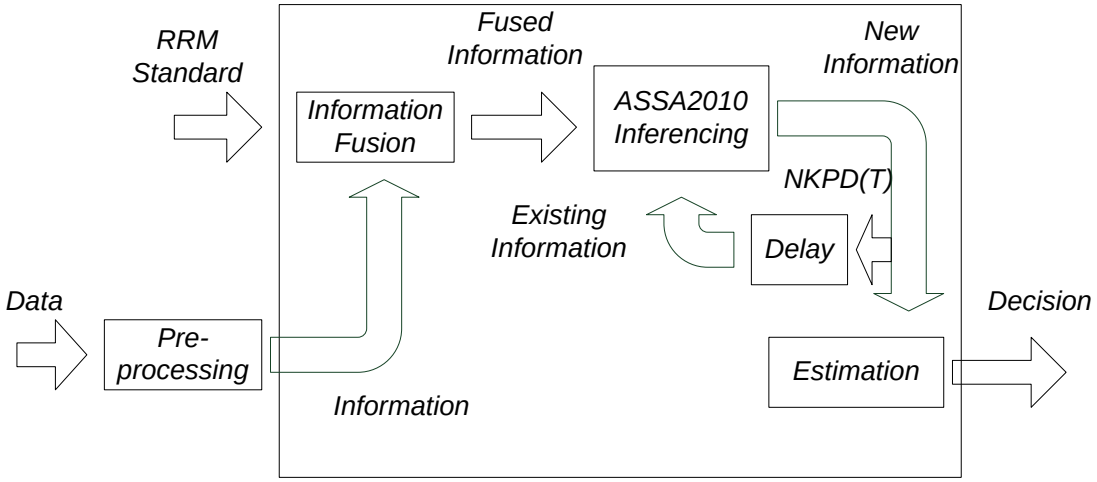

Figure 2. Diagram of the proposed method

CAI is derived from Bayesian Inference Method (BIM) and is shown in equation (4) [9], [12].

$$\square(\square_{\square}|\square_{\square}) = \sum_{\square=1}^{\square}\left(\frac{\square(\square_{\square}|\square_{\square})\square(\square_{\square})}{\sum_{\square=1}^{\square}\square(\square_{\square}|\square_{\square})\square(\square_{\square})}\right) \quad (4)$$

Where P(Bj|Ai) is the probability of Possible Fault (PF) Bj given the indication Ai, P(Ai|Bj) is the probability of Indication Ai given PF Bj. P(Bj) is the probability of PF Bj, and Σ(P(Ai|Bk) P(Bk) is the probability combination of all PF. They are arranged in the observation matrix as fused information (P(υij)) [13].

Fused informations are used to form New Knowledge Probability Distribution (NKPD). It is the probability of each PF considering all indications, as is shown in equation (5) [13].

$$\square\left(\square_{\square}^{\square}\right) = \frac{\sum_{\square=1}^{\square}\square(\square_{\square}^{\square})}{\square} \quad (5)$$

Where δ indicates the number of sensors and P(ψij) indicates the inferenced fused-information. For time-independent observation, NKPD will not be fused with the previous NKPD. The next process is calculating Degree of Certainty (DoC) of each PF shown in equation (6) [12].

$$\square\square\square = \square\square\square[\square(\square_{\square})] \quad (6)$$

Where j = 1, 2, 3, …, λ. Is the number of possible fault.

CAI-based RRM uses the same indications and PF as conventional one does. Indications are fused with standard to obtain information with Degree of Certainty (DoC) [13].

3. Result and Analysis

The proposed method is verified using IEC TC10 labeled dataset consists of nine samples PD, 26 samples LE, 48 samples HE, 16 samples TL, and 18 samples TH. Data example for Low-Energy Discharge is shown in Table 3.

RRM works on Ratios, the next step is to calculate R_1, R_2, and R_5 using equation (1) to equation (3) and localized them. The result is shown in Table 4 [14, p. 104]. For sample 1, R_1 = 0.256, and therefore Localized R_1 = "0". R_2 = 2.154, and therefore localized R_2 = "1". R_5 = 1.182, and therefore localized R_5 = "1". Sample 2 shows R_1, R_2, and R_5 are

0.328, 3.360, and 4.879 respectively, and therefore localized R_1, R_2, and R_5 are "0", "2", and "2" respectively.

Table 3. DGA data for Low-Energy Discharge .

No.	H2	CH4	C2H6	C2H4	C2H2	CO	CO2	TCG
1	78	20	11	13	28	0	784	150
2	305	100	33	161	541	440	3700	1580
3	35	6	3	26	482	200	2240	752
…	…	…	…	…	…	…	…	…
24	1900	285	31	957	7730	681	732	11584
25	57	24	2	27	30	540	2518	680
26	1000	500	1	400	500	200	1000	2601

The observation matrix is created localized ratios are put in the observation matrix as shown in Table 5. For the sample 1, R_1 = "0", using Table 1, LE = "1" can be calculated. R_2 = "1", using Table 1, all Possible Faults (PF) = '1' and can be calculated. R_5 = "1", using Table 1, TL and TH are "1".

The probability of every PF considering all indication is calculated using equation (5), resulting DoC and is shown in Table 6. For sample no. 1, the DoC of LE, HE, TL, and TH are 0.417, 0.083, 0.250, and 0.250 respectively. Fault type LE has the most Degree of Certainty (DoC) in sample 1. It indicates that LE was the most occurred fault before the observation takes place. In sample 2, the DoC of LE, HE, TL, and TH are 0.444, 0.000, 0.111, and 0.444 respectively. LE and TH have the most DoC. it indicates that LE and TH were the most faults occurred before the observation take place. The other samples are analyzed using the same method.

Overall accuracy of the proposed method is shown in Table 7. CAI is used to analyzed 117 samples consists of 9 PDs, 26 LEs, 48 HEs, 16 TLs, and 18 THs. CAI performs over-all accuracy of 45.3%, with varies accuracies between fault types. CAI has the accuracy of 44.44% when is used to identify PD, 92.31% accuracy when is used to identify LE, 12.5% accuracy when is used to identify HE, 6.25% accuracy when is used to identify TL, and 100% accuracy when is used to identify TH.

Table 4. Ratios and localized Ratios: R_1, R_2, and R_5.

No. Obs.	Ratio			Localized Ratio		
	R_1	R_2	R_5	R_1	R_2	R_5
1	0.256	2.154	1.182	0	1	1
2	0.328	3.360	4.879	0	2	2
3	0.171	18.538	8.667	0	2	2
…	…	…	…	…	…	…
24	0.150	8.077	30.871	0	2	2
25	0.421	1.111	13.500	0	1	2
26	0.500	1.250	400.000	0	1	2

Table 5. Observation Matrix.

No. Obs.	Ratios	score	Possible Fault			
			LE	HE	TL	TH
1	R_1	0	1	0	0	0
	R_2	1	1	1	1	1
	R_5	1	0	0	1	1
2	R_1	0	1	0	0	0
	R_2	2	1	0	1	1
	R_5	2	0	0	0	1
3	R_1	0	1	0	0	0
	R_2	2	1	0	1	1
	R_5	2	0	0	0	1
…	…	…	…	…	…	…
24	R_1	0	1	0	0	0
	R_2	2	1	0	1	1
	R_5	2	0	0	0	1
25	R_1	0	1	0	0	0
	R_2	1	1	1	1	1
	R_5	2	0	0	0	1
26	R_1	0	1	0	0	0
	R_2	1	1	1	1	1
	R_5	2	0	0	0	1

Table 6. NKPD.

No.	LE	HE	TL	TH
1	0.417	0.083	0.250	0.250
2	0.444	0.000	0.111	0.444
3	0.444	0.000	0.111	0.444
…	…	…	…	…
24	0.444	0.000	0.111	0.444
25	0.417	0.083	0.083	0.417
26	0.417	0.083	0.083	0.417

Table 7. Overall Accuracy of CAI.

Fault	Sample	Accurate	%Accuracy
PD	9	4	44.44
LE	26	24	92.31
HE	48	6	12.50
TL	16	1	6.25
TH	18	18	100.00
Total	117	53	45.30

ISSN: 2005-4238 IJAST

CAI results is tested using Fuzzy Inference System (FIS) and Artificial Neural Network (ANN) as existing AI methods, and compared using enhancement from previous researches. The result is shown in Table 8.

Both comparison methods use the same data. FIS used three-ratio input, four-PF output and a set of rules. Input and output membership functions are shown in Table 9.

Table 8. Accuracy of CAI compared to other methods.

Fault Type	Accuracy (%)					
	Rogers	Taha	Duval	FIS	ANN	CAI
	[15]					
PD	58.33	58.33	37.5	55.56	85.2	44.44
LE	47.16	56.6	62.26	3.85	69.71	92.31
HE	7.4	67.59	69.4	100	93.75	12.5
TL	92.31	92.31	52.56	6.25	75	6.25
TH	48	100	96	88.89	72.22	100

Table 9. FIS parameter

In/ out	Low		Med		High	
	Type	Parameter	Type	Parameter	Type	Parameter
R_1	Sigmoid	[-3.829 0.2]	Gaussian	[0.5 0.55]	Sigmoid	[2.641 1]
R_2	Sigmoid	[-1.5 0.1]	Gaussian	[1.06 1.55]	Sigmoid	[1.666 3]
R_5	Sigmoid	[-2.16 1]	Gaussian	[1 2]	Sigmoid	[2 3]
PD	Sigmoid	[0.2123 0]	Gaussian	[0.2123 0.5]	Sigmoid	[0.2123 1]
LE	Sigmoid	[0.2123 0]	Gaussian	[0.2123 0.5]	Sigmoid	[0.2123 1]
HE	Sigmoid	[0.2123 0]	Gaussian	[0.2123 0.5]	Sigmoid	[0.2123 1]
TL	Sigmoid	[0.2123 0]	Gaussian	[0.2123 0.5]	Sigmoid	[0.2123 1]
TH	Sigmoid	[0.2123 0]	Gaussian	[0.2123 0.5]	Sigmoid	[0.2123 1]

Due to the large number of data required by ANN, 10-fold cross validation method is used. The number of node in hidden layer is determined using Gaussian approximation in (7).

$$□(□) = □ \times □^{-(□-□/□)^2} \quad (7)$$

Where a is the predicted maximum accuracy, b is the optimum node, and c is the sensitivity. Several number of node with 50 training each node resulting:

$$a = 74.45 \quad (8)$$

$$b = 378 \quad (9)$$

$$c = 1862 \quad (10)$$

The three type of AI has different characteristics. CAI has the most accuracy in identifying LE and TH, ANN has higher accuracy in identifying PD and, while FIS has the most accuracy in identifying HE. ANN has the most overall accuracy due to the 10-fold cross validation method. FIS has the average accuracy, and CAI has the least overall accuracy in adopting RRM.

Compared to other method, CAI has some advantages. CAI identifies LE more accurate, while Taha's method of improving RRM identifies TL more accurate. Both methods perform the same accurate identification if used to identify TH.

4. Concluding Remarks

CAI is the novel method in transformer fault identification by fusing informations from various sensors and producing new information that is used to make decisions. CAI is capable of adopting existing conventional methods of fault identification. Compared to FIS and ANN, CAI for RRM has the lowest overall accuracy, but using CAI on RRM has the most accuracy for LE and TH.

The accuracy of the proposed method can be increased using the combination of several methods [16], [17]. DGA data will be identified using several method and given weight score according to its accuracy in identifying each fault [16], [17]. The proposed method for RRM will be enhanced with Fuzzy [18] and will be used to estimate transformer remaining life [19], [20]. The other area of implementation will be in biomedic [21], [22], prediction and classifier [23], data analysis in cloud [24], network intrusion detection system in [25], and in the hardware security [26]. CAI may also works together with numerical simulation [27] and the area of optimization in renewable energy [28], [29].

Acknowledgments

The first author would like to show his gratitude to Prof. Adang Suwandi Ahmad, who, although no longer with us, continues to inspire by his dedication to develop cognitive intelligent instrumentation science and engineering.

References

[1] ABB, "Transformer Handbook." ABB, 2004.
[2] H. Das, K. Gogoi, and S. Chatterjee, "Analysis of the effect of electric field due to High Voltage Transmission lines on humans," in *2015 1st Conference on Power, Dielectric and Energy Management at NERIST (ICPDEN)*, Itanagar, India, Jan. 2015, pp. 1–4, doi: 10.1109/ICPDEN.2015.7084491.
[3] F. D. Samirmi, W. Tang, and Q. Wu, "Fuzzy Ontology Reasoning for Power Transformer Fault Diagnosis," *AECE*, vol. 15, no. 4, pp. 107–114, 2015, doi: 10.4316/AECE.2015.04015.
[4] M. J. Heathcote and D. P. Franklin, *The J & P transformer book: a practical technology of the power transformer*, 12th ed. Oxford ; Boston: Newnes, 1998.
[5] "An American National Standard IEEE Guide for the Detection and Determination of Generated Gases in Oil-Immersed Transformers and their Relation to the Serviceability of the Equipment," ANSI/IEEE, 1978.
[6] *Facilities Instructions, Standards, and Techniques*, vol. 3–31. United States Department of the Interior Bureau of Reclamation, 2003.
[7] R. Nidhiritdhikrai, K. Audomvongseree, and B. Eua-arporn, "Loss assessment in a low-voltage distribution system," in *2009 6th International Conference on Electrical Engineering/Electronics, Computer, Telecommunications and Information Technology*, Chonburi, Thailand, May 2009, pp. 10–13, doi: 10.1109/ECTICON.2009.5136955.
[8] Cigre Working Group 12.18, "Guidelines for Life Management Techniques for Power Transformers." Cigre.
[9] K. O. Bachri, U. Khayam, B. A. Soedjarno, A. D. W. Sumari, and A. S. Ahmad, "Cognitive artificial-intelligence for doernenburg dissolved gas analysis interpretation," *TELKOMNIKA*, vol. 17, no. 1, p. 268, Feb. 2019, doi: 10.12928/telkomnika.v17i1.11612.
[10] "IEEE Guide for the Interpretation of Gases Generated in Mineral Oil-Immersed Transformers," IEEE. doi: 10.1109/IEEESTD.2019.8890040.
[11] M. Duval and A. dePabla, "Interpretation of gas-in-oil analysis using new IEC publication 60599 and IEC TC 10 databases," *IEEE Electr. Insul. Mag.*, vol. 17, no. 2, pp. 31–41, Mar. 2001, doi: 10.1109/57.917529.
[12] A. D. W. Sumari, A. S. Ahmad, A. I. Wuryandari, and J. Sembiring, "Constructing Brain-Inspired Knowledge- Growing System: A Review and A Design Concept."
[13] A. D. W. Sumari and A. S. Ahmad, "Knowledge-growing system: The origin of the cognitive artificial intelligence," in *2017 6th International Conference on Electrical Engineering and Informatics (ICEEI)*, Langkawi, Nov. 2017, pp. 1–7, doi: 10.1109/ICEEI.2017.8312382.
[14] "IEEE Guide for the Interpretation of Gases Generated in Oil - Immersed Transformers," Feb. 2019.
[15] I. B. M. Taha, Sherif. S. M. Ghoneim, and H. G. Zaini, "Improvement of Rogers four ratios and IEC Code methods for transformer fault diagnosis based on Dissolved Gas Analysis," in *2015 North American Power Symposium (NAPS)*, Charlotte, NC, USA, Oct. 2015, pp. 1–5, doi:

10.1109/NAPS.2015.7335098.
[16] G. K. Irungu, A. O. Akumu, and J. L. Munda, "Transformer condition assessment for maintenance ranking: A comparison of three standards and different weighting techniques," in *2017 IEEE AFRICON*, Cape Town, Sep. 2017, pp. 1043–1048, doi: 10.1109/AFRCON.2017.8095626.
[17] T. Trianto, S. Suwarno, Y. Li, and Z. Guan-Jun, "Combining conventional and artificial intelligence DGA interpretation methods using optimized weighting factor.pdf," presented at the 2016 International Seminar on Intelligent Technology and Its Application, Lombok, Indonesia, pp. 37–42, doi: 10.1109/ISITIA.2016.7828630.
[18] K. O. Bachri, B. Anggoro, and A. S. Ahmad, "Interpreting DGA Key Gas using Fuzzy OMA3S," in *2016 International Symposium on Electronics and Smart Devices (ISESD)*, Bandung, Indonesia, Nov. 2016, pp. 137–142, doi: 10.1109/ISESD.2016.7886707.
[19] K. O. Bachri, B. Anggoro, and A. S. Ahmad, "Transformer performance calculation using information fusion based on DGA interpretation," in *2016 International Symposium on Electronics and Smart Devices (ISESD)*, Bandung, Indonesia, Nov. 2016, pp. 11–15, doi: 10.1109/ISESD.2016.7886756.
[20] K. O. Bachri, B. Anggoro, A. D. W. Sumari, and A. S. Ahmad, "Cognitive Artificial Intelligence Method for Interpreting Transformer Condition Based on Maintenance Data," *Adv. sci. technol. eng. syst. j.*, vol. 2, no. 3, pp. 1137–1146, Jul. 2017, doi: 10.25046/aj0203143.
[21] L. Goeirmanto, R. Mengko, and T. L. Rajab, "Direction of ventricle contraction based on precordial lead ECG signal," in *2016 4th International Conference on Cyber and IT Service Management*, Bandung, Indonesia, Apr. 2016, pp. 1–3, doi: 10.1109/CITSM.2016.7577572.
[22] C. O. Sereati, A. D. W. Sumari, T. Adiono, and A. S. Ahmad, "Cognitive artificial intelligence (CAI) software based on knowledge growing system (KGS) for diagnosing heart block and arrythmia," presented at the 2017 6th International Conference on Electrical Engineering and Informatics (ICEEI), Langkawi, Malaysia, pp. 1–5, doi: 10.1109/ICEEI.2017.8312368.
[23] N. A. A. Ansari, S. Nandgave, M. Ansari, and S. Gupta, "Heart Disease Prediction Using Machine Learning Classifiers," *International Journal of Advanced Science and Technology*, vol. 29, no. 6, p. 8, 2020.
[24] F. Zulkernine, P. Martin, Y. Zou, M. Bauer, F. Gwadry-Sridhar, and A. Aboulnaga, "Towards Cloud-Based Analytics-as-a-Service (CLAaaS) for Big Data Analytics in the Cloud," in *2013 IEEE International Congress on Big Data*, Santa Clara, CA, USA, Jun. 2013, pp. 62–69, doi: 10.1109/BigData.Congress.2013.18.
[25] H. R. A. Talompo, A. S. Ahmad, Y. S. Gondokaryono, and S. Sutikno, "NAIDS design using ChiMIC-KGS," in *2017 International Symposium on Electronics and Smart Devices (ISESD)*, Yogyakarta, Oct. 2017, pp. 346–351, doi: 10.1109/ISESD.2017.8253362.
[26] S. D. Putra, A. S. Ahmad, S. Sutikno, Y. Kurniawan, and A. D. W. Sumari, "Revealing AES Encryption Device Key on 328P Microcontrollers with Differential Power Analysis," *IJECE*, vol. 8, no. 6, p. 5144, Dec. 2018, doi: 10.11591/ijece.v8i6.pp5144-5152.
[27] S. T. Ahmed, R. S. Mehsen, and T. H. Hadi, "A Structural Model Fuzzy Multiple Regression Analysis to Cloud Computing Security Issues," *IJAST*, vol. 29, no. 3, pp. 809–825, 2020.
[28] S. B. Dubey, A. Tripathi, and B. Dwivedi, "Implementation of Smart Grid Concept in Interconnection of Micro Grid and Power Grid," *International Journal of Advanced Science and Technology*, vol. 29, no. 6, p. 7, 2020.
[29] T. Nur and Herlina, "Enhancement of Cogging Torque Reduction on Inset Permanent Magnet Generator by Using Magnet Edge Shaping Method," in *2018 International Conference on Electrical Engineering and Computer Science (ICECOS)*, Pangkal Pinang, Oct. 2018, pp. 429–434, doi: 10.1109/ICECOS.2018.8605247.